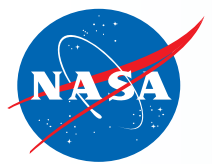


Acoustic Mode Decomposition in Rectangular Ducts with Sheared Flow

**Alexander N. Carr
NASA Langley Research Center, Hampton, VA**

**30th AIAA/CEAS Aeroacoustics Conference
Rome, Italy
June 7, 2024**

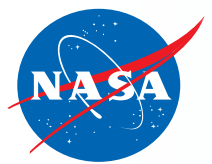


Acknowledgments

This work was funded by the Advanced Air Transport Technology Project under the Advanced Air Vehicles Program at the National Aeronautics and Space Administration.

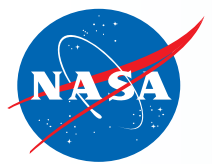


Thanks to Doug Nark, Mike Jones, Jason June, Max Reid, Martha Brown and Brian Howerton for input and feedback.



Motivation

- Acoustic liner design and optimization becoming more important as bypass ratio increases
- Design, optimization, and verification process often relies upon Ingard-Myers BC (see [1, 2])
- Assumes infinitesimal thickness of boundary layer, maybe okay for large bypass duct, but not okay for small cross-section test rig (Grazing Flow Impedance Tube, GFIT, is 2 x 2.5 in)
- Flow in test rigs is highly 3D, e.g., the Curved Duct Test Rig (CDTR) cross-section (15 x 6 in) is 40% boundary layer
- Why is this important?
 - Always working to improve liner design and optimization
 - Desire to test up to 6 kHz in Liner Technology Facility (LTF); shear layer refraction will be increasingly important
 - Improve our physical understanding of impedance BC in shear flow and address questions regarding flow direction effects
- Thus, higher fidelity analysis methods that incorporate 3D shear flow refraction should be explored



Objectives

Challenges and Questions to Address

- Developing impedance reduction technique with 3D shear flow is a big challenge
- Natural first step: mode decomposition with 3D shear flow effects
- Are plane-wave or higher-order modes more sensitive to shear flow refraction effects? [3, 4]
- How does the acoustic propagation direction relative to flow direction affect acoustic modes? [5]

Objectives

- Develop mode decomposition procedure based upon the Pridmore-Brown Eqn. (PBE) for 3D sheared duct flow
- Investigate the effect of flow direction on the mode structure, propagation, and amplitudes
- Examine sensitivity of lower- and higher-order modes to shear flow

Process

- CDTR already has Convective Helmholtz Eqn. (CHE) mode decomposition capabilities
- Ideal test bed for a higher-fidelity mode decomposition study
- Flow survey performed to extract flow profile
- Acoustic study with two different liner samples performed at three different centerline Mach numbers

Governing Equation

- Pridmore-Brown Equation (PBE) [6]

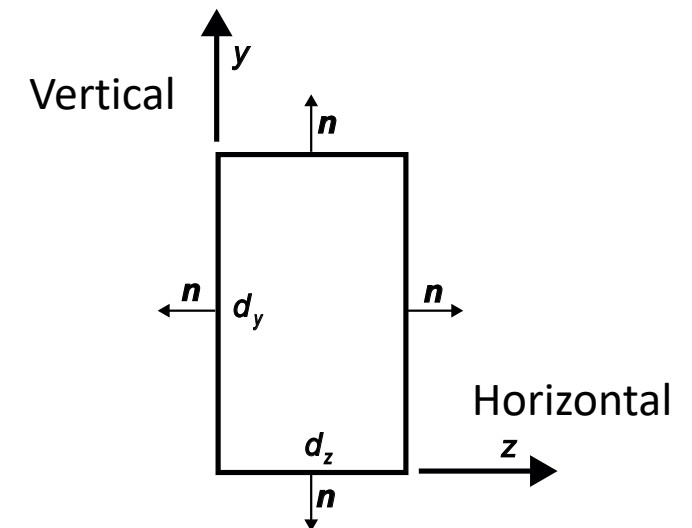
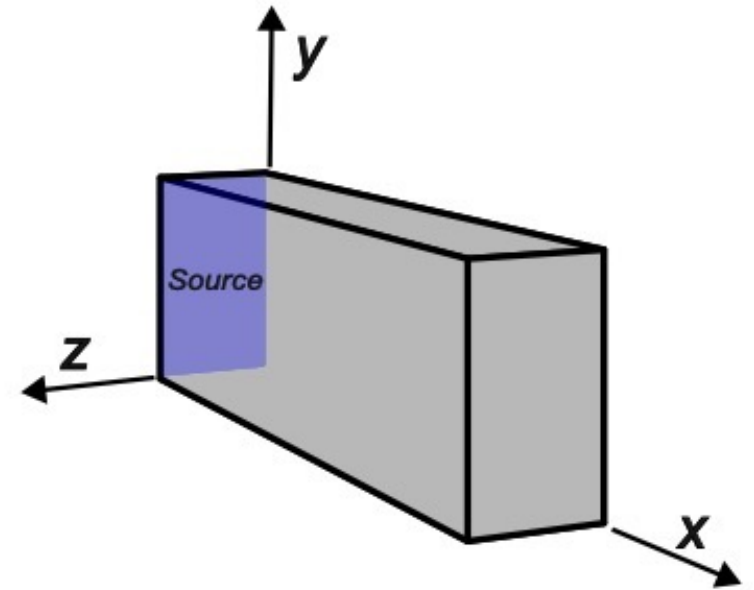
$$(k - \kappa M)^2 \nabla \cdot \left(\frac{1}{(k - \kappa M)^2} \nabla \hat{p} \right) + [(k - \kappa M)^2 - \kappa^2] \hat{p} = 0 \quad (1)$$

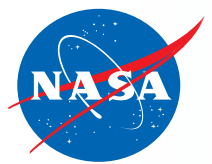
$$p(x, y, z, t) = \hat{p}(y, z; \kappa, \omega) \exp(-i\omega t + i\kappa x)$$

- Ingard-Myers boundary condition ([1, 2])

$$\nabla \hat{p} \cdot \mathbf{n} + \frac{(k - \kappa M)^2}{ik\zeta} \hat{p} = 0 \quad (2)$$

- No slip, $M = 0$ at walls
- No straightforward dispersion relation for κ in nonuniform flow
- Set up an eigenvalue problem to determine κ (approach based upon Rienstra [7])
- Notation: CHE modes will be in (vertical, horizontal) format when discussed in presentation





Galerkin Projection

- Multiply Eqn. 1 by $\phi(k - \kappa M)^{-2}$ and integrate over cross-section (Assume hardwall BC for brevity)

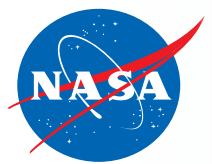
$$\int_0^{d_z} \int_0^{d_y} \frac{(\nabla\phi \cdot \nabla\hat{p})}{(k - \kappa M)^2} - \left[1 - \frac{\kappa^2}{(k - \kappa M)^2} \right] \phi\hat{p} dy dz = 0 \quad (3)$$

- Assume a form of the solution

$$\hat{p} = \sum_{n=0}^{\infty} \sum_{m=0}^{\infty} a_{mn} \psi_{mn}(y, z) \quad (4)$$

- Let $\psi_{mn}(y, z) = T_m(\tilde{y})T_n(\tilde{z})$, where \tilde{y} and \tilde{z} are normalized to the range -1 to +1
- $\phi = \psi_{m'n'}$
- Results in a matrix equation ($\mathcal{M}(\kappa)$ described in paper)

$$\mathcal{M}(\kappa)\mathbf{a} = 0 \quad (5)$$



Method of Successive Linear Problems

- Eqn. (5) is a nonlinear eigenvalue problem for (κ, \mathbf{a})
- Need to find all (κ, \mathbf{a}) pairs that satisfy the Galerkin projection
- Linearize about the point μ

$$\mathcal{M}(\kappa) = \mathcal{M}(\mu) + (\kappa - \mu) \boxed{\left. \frac{d\mathcal{M}}{d\kappa} \right|_{\kappa=\mu}} \quad \mathcal{M}'(\mu) \quad (6)$$

- Approximate eigenvalue problem by the linearization (Method of Successive Linear Problems, MSLP, see [8, 9])

$$\mathcal{M}(\kappa)\mathbf{a} \approx [\mathcal{M}(\mu) + (\kappa - \mu)\mathcal{M}'(\mu)]\mathbf{a} = 0 \quad (7)$$

- Process to find κ :
 1. Make initial guess, μ_0
 2. Iterate on the generalized eigenvalue problem, $\mathcal{M}(\mu)\mathbf{x} = -\lambda\mathcal{M}'(\mu)\mathbf{x}$
 3. Set $\mu = \mu_0 + \lambda$ and check convergence
 4. If not converged, use μ as new guess; if converged, set $\kappa^{(j)} = \mu$ and $\mathbf{a}^{(j)} = \mathbf{x}$



Modal Analysis

- Acoustic pressure field may be expressed as

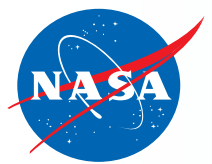
$$P(x, y, z; \omega) = \sum_{j=1}^J \chi_j \overbrace{\sum_{n=0}^{\tilde{N}} \sum_{m=0}^{\tilde{M}} a_{mn}^{(j)} \psi_{mn}(y, z) e^{i\kappa^{(j)}x}}^{\hat{p}_j} \quad (8)$$

- χ_j are the complex mode coefficients
- Microphone measurements provide $P(x, y, z; \omega)$ at specific in-duct locations
- Then, linear least-squares regression may be used to determine χ_j
- Once χ_j are determined, the following quantities are of interest
 - Mode SPL, $\text{SPL}_{\text{mode},j} = 10 \log \left(\frac{\chi_j \chi_j^*}{2p_{\text{ref}}^2} \right)$
 - Reconstruction error in SPL and phase

$$E_{\text{SPL,PBE}} = \frac{\|\text{SPL}_{\text{PBE}} - \text{SPL}_{\text{measured}}\|_2}{\|\text{SPL}_{\text{measured}}\|_2}$$

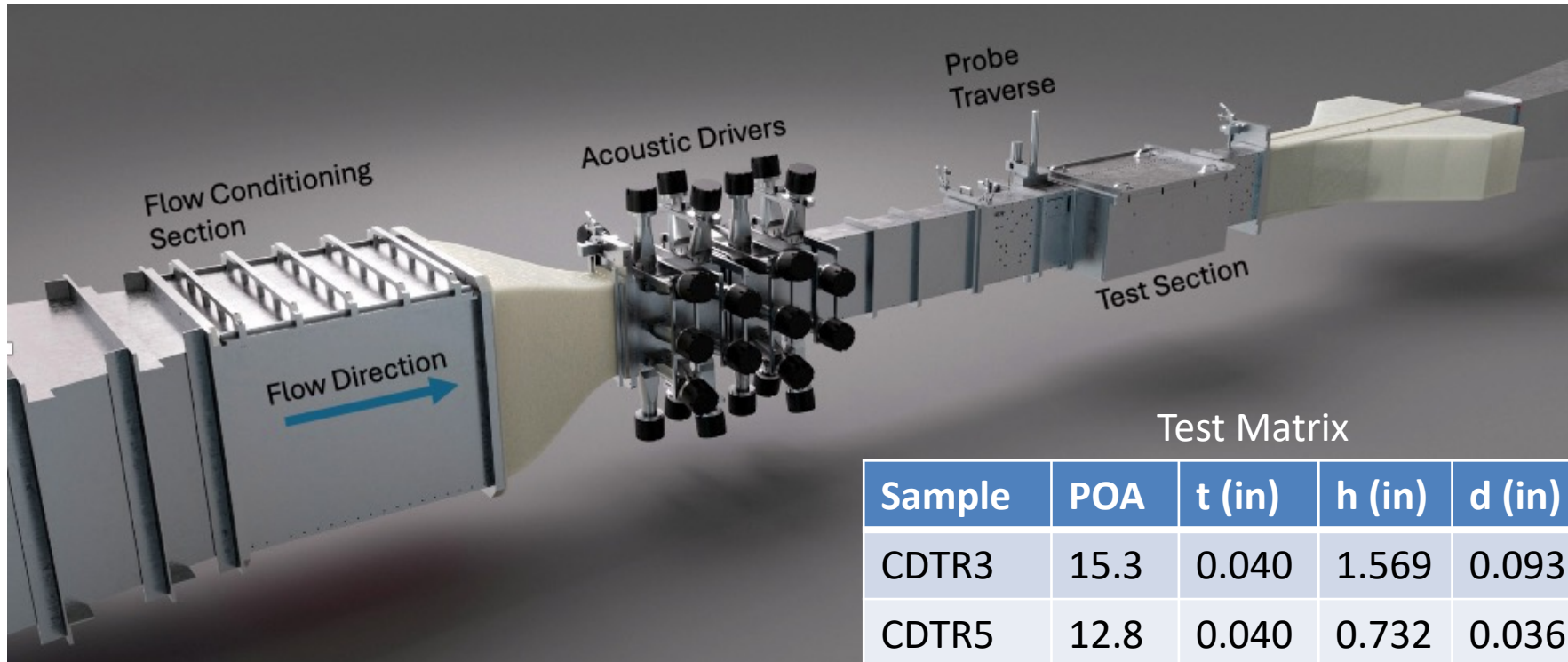
$$E_{\text{phase,PBE}} = \frac{1}{N_{\text{mics}}} \sum_{i=1}^{N_{\text{mics}}} \frac{\min(s, s^c)}{\pi} \quad (9a,9b)$$

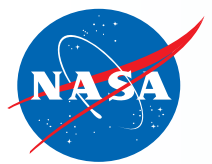
$$s = |\theta_{\text{measured}} - \theta_{\text{PBE}}|$$



Experimental Setup

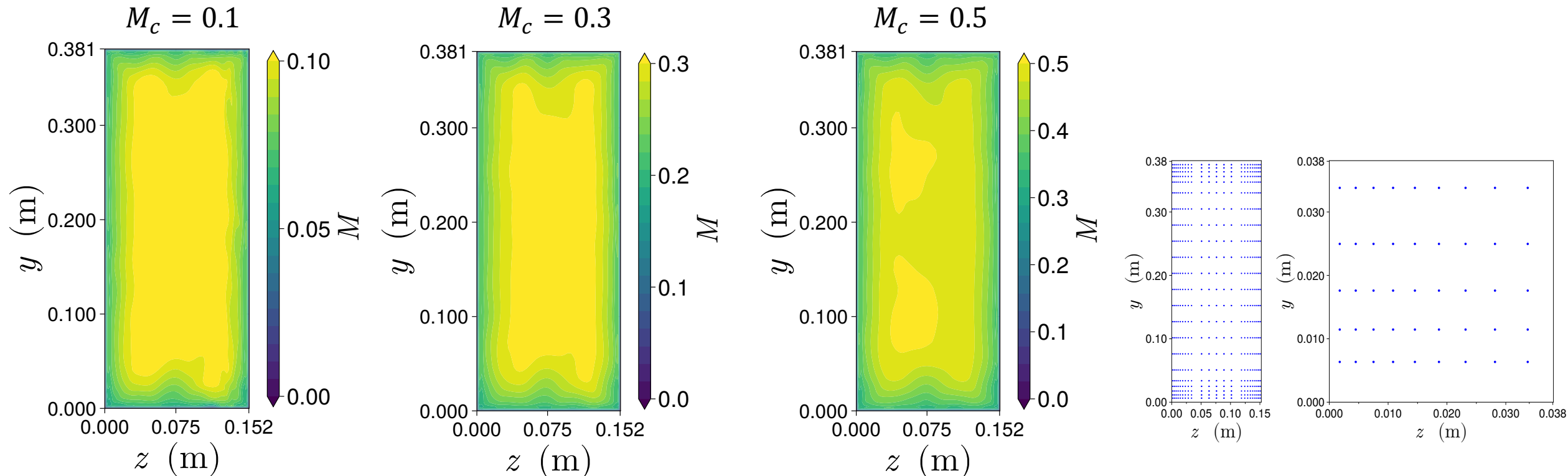
- Curved Duct Test Rig (CDTR) – open-loop wind tunnel capable of $M_c = 0.5$ in test section
- 15 x 6 in test section
- 32 acoustic drivers – mode control
- Probe traverse for flow measurements along cross-section before and after test section
- Test matrix: CDTR3 and CDTR5 liner samples at $M_c = 0.1, 0.3,$ and 0.5





Flow Measurements

- Total pressure probe to measure Mach number upstream of test section
- Downstream measurements could not be performed due to fan bearing seal failure
- NURBS surface constructed from measurements, then Mach number interpolated onto Legendre points for quadrature

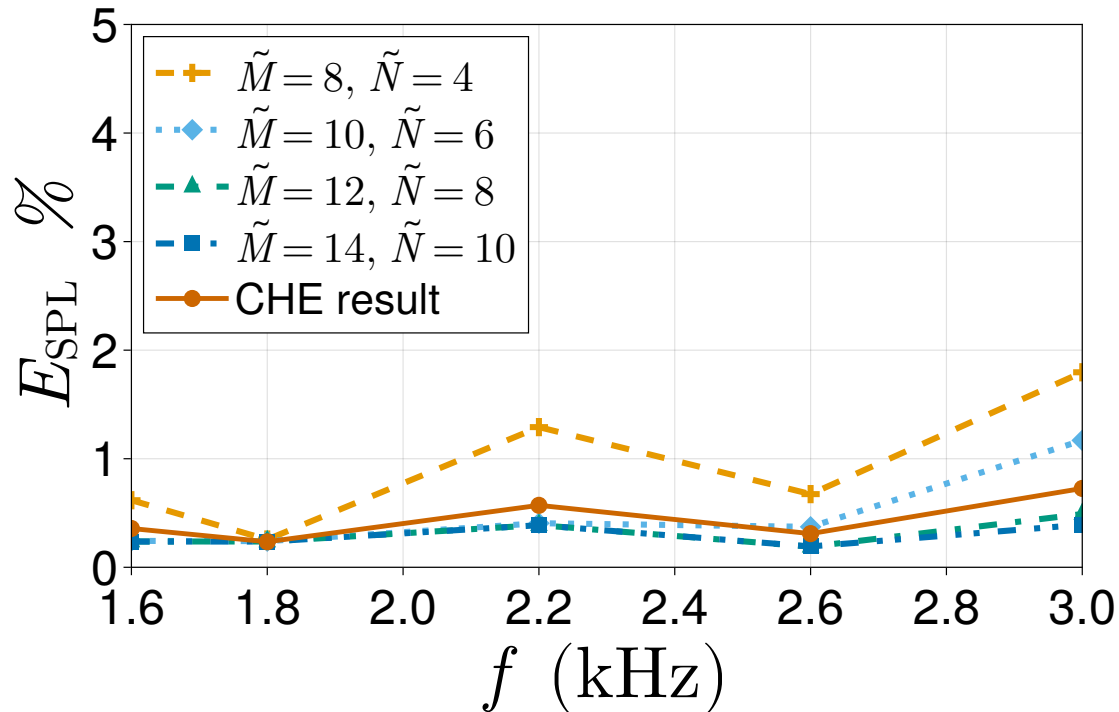




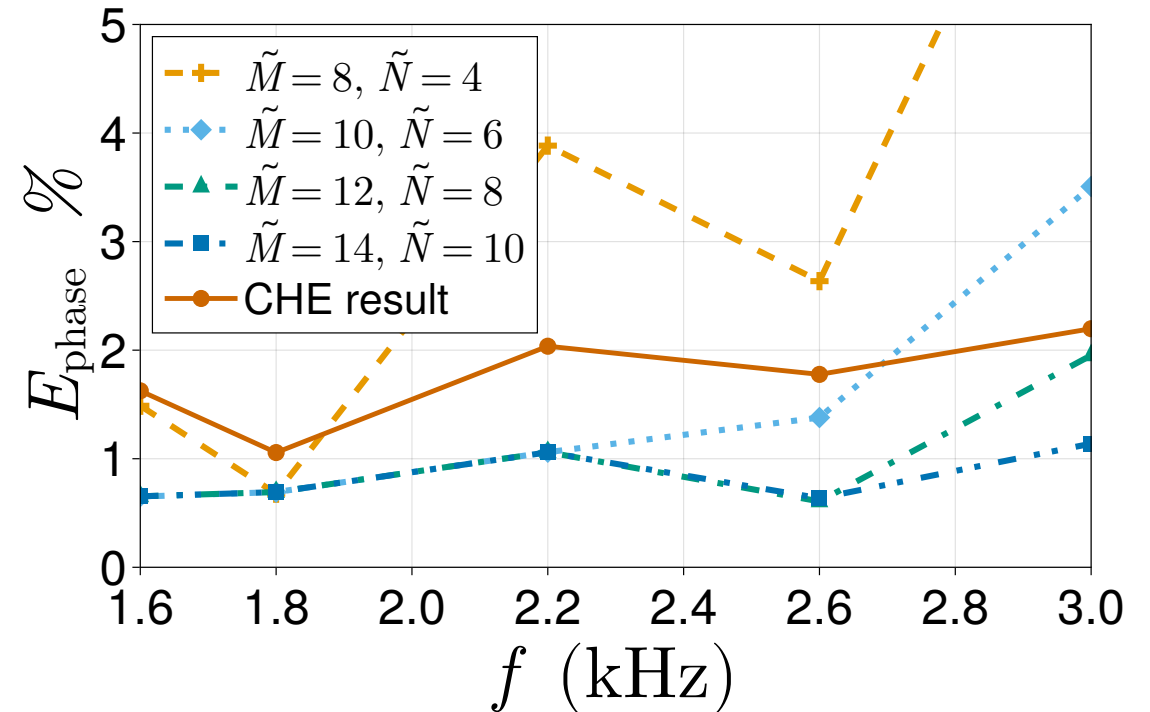
Reconstructed Sound Field

- With knowledge of Mach number at quadrature points, we may now solve $\mathcal{M}(\kappa)\mathbf{a} = 0$ and compute the PBE modes
- Validation: compare reconstruction error of PBE modes with traditional CHE modes
- Results show lower reconstruction error for PBE modes as \tilde{M} and \tilde{N} are increased

SPL Reconstruction Error, $M_c = 0.5$ and κ_4 mode



Phase Reconstruction Error, $M_c = 0.5$ and κ_4 mode



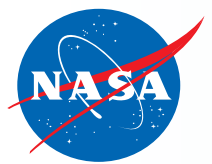


Wavenumber Deviations

- Number of eigenvalues found for PBE modes is generally equal to number of wavenumbers for CHE modes
- No significant wavenumber deviations resulting from shear flow for $M_c = 0.1$ and 0.3
- For $M_c = 0.5$, negative modes are more significantly impacted than positive modes
- Absolute value of wavenumber is smaller for PBE modes propagating against the flow

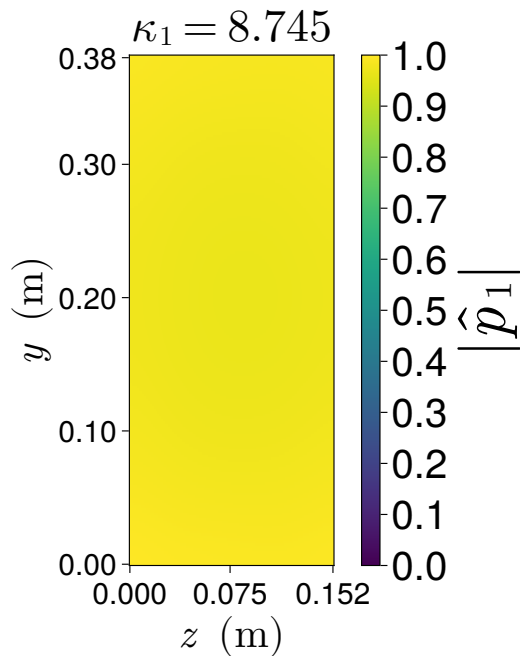
$$M_c = 0.5$$

PBE mode #	CHE mode #	κ , PBE	κ , CHE
1	(0,0)	20.750	20.148
2	(1,0)	19.736	19.005
3	(2,0)	15.938	15.356
7	(2,1)	6.598	6.168
8	(3,1)	-5.638	-4.755
9	(4,0)	-8.511	-7.173
-9	-(4,0)	-25.340	-32.801
-8	-(3,1)	-25.965	-35.219
-7	-(2,1)	-37.798	-46.142
-3	-(2,0)	-48.780	-55.331
-2	-(1,0)	-53.020	-58.980
-1	-(0,0)	-55.658	-60.122

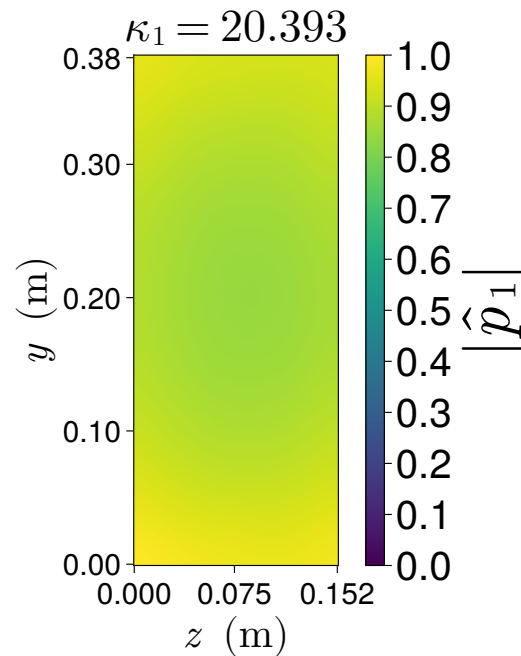


Modal Structure

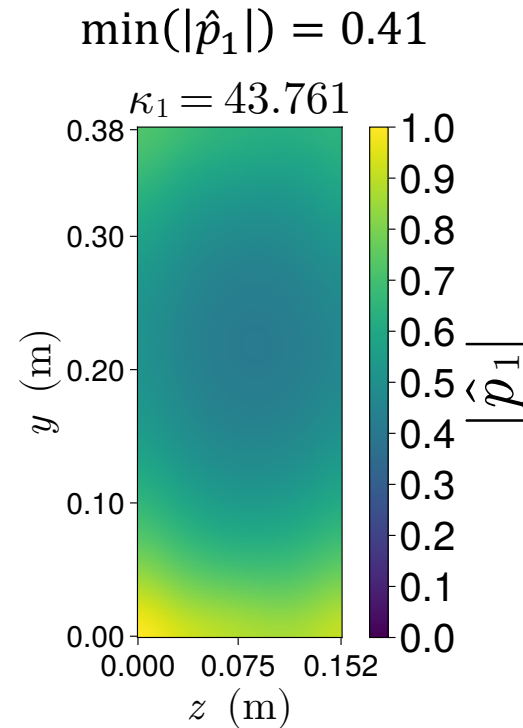
- As frequency and Mach number increase, modal structure becomes more “distorted” relative to traditional CHE mode structure
- Lowest-order mode becomes increasingly non-planar as flow speed and frequency increase (shown below)
- Asymmetry between positive and negative mode structures also present (shown on next slide)
- Lowest-order mode is first mode to exhibit this asymmetry (discussed in paper)



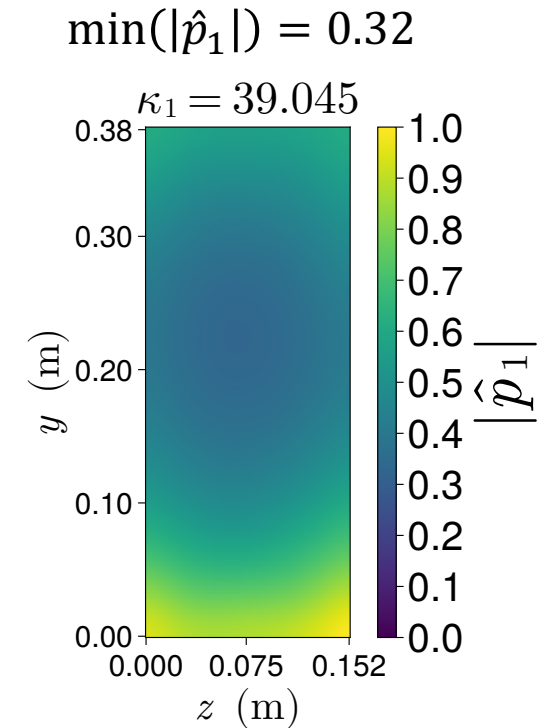
$f = 600$ Hz and $M_c = 0.3$



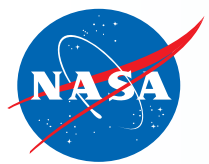
$f = 1400$ Hz and $M_c = 0.3$



$f = 3000$ Hz and $M_c = 0.3$



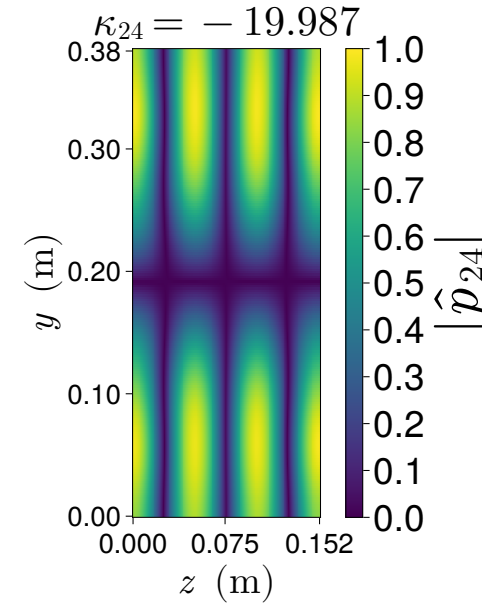
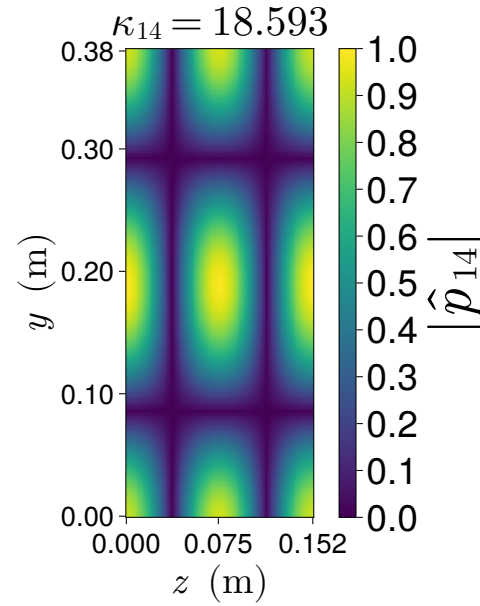
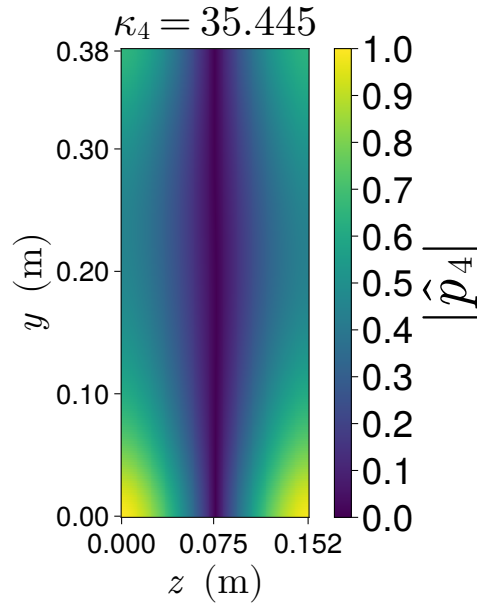
$f = 3000$ Hz and $M_c = 0.5$



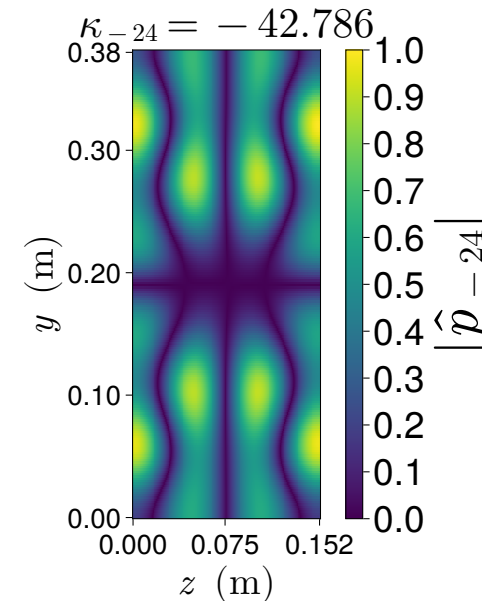
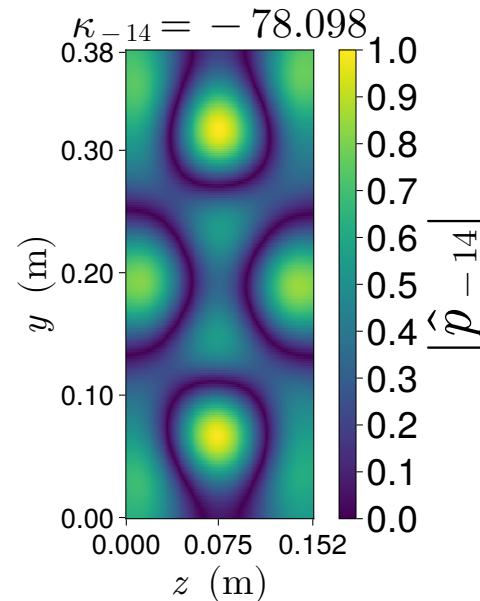
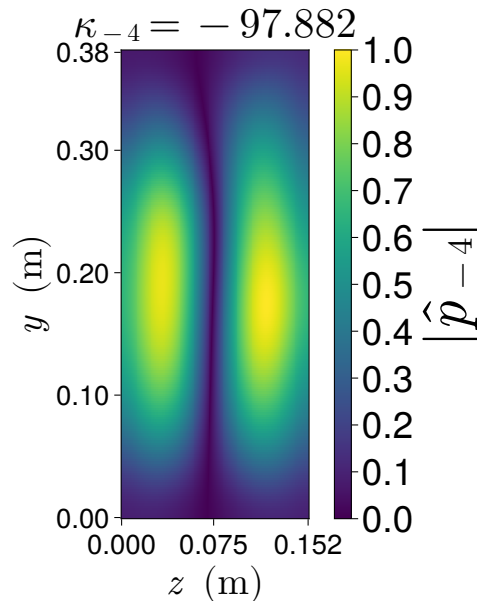
Modal Structure (Flow Direction Effects)

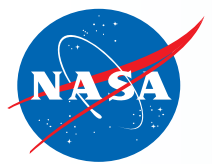
$f = 3000$ Hz and
 $M_c = 0.5$

Positive
Modes



Negative
Modes





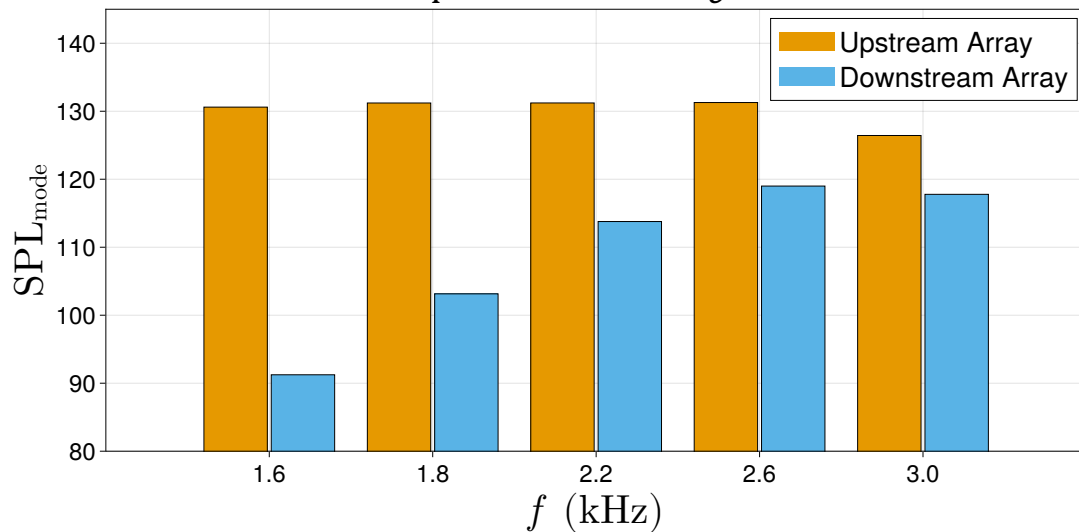
Mode SPL

- Mode SPL upstream and downstream of two liner samples computed using PBE and CHE modes
- Very good agreement for lowest-order mode
- More noticeable disagreement for higher-order modes, but CHE results may still be acceptable for design purposes
- Insensitive to Mach number, surprisingly

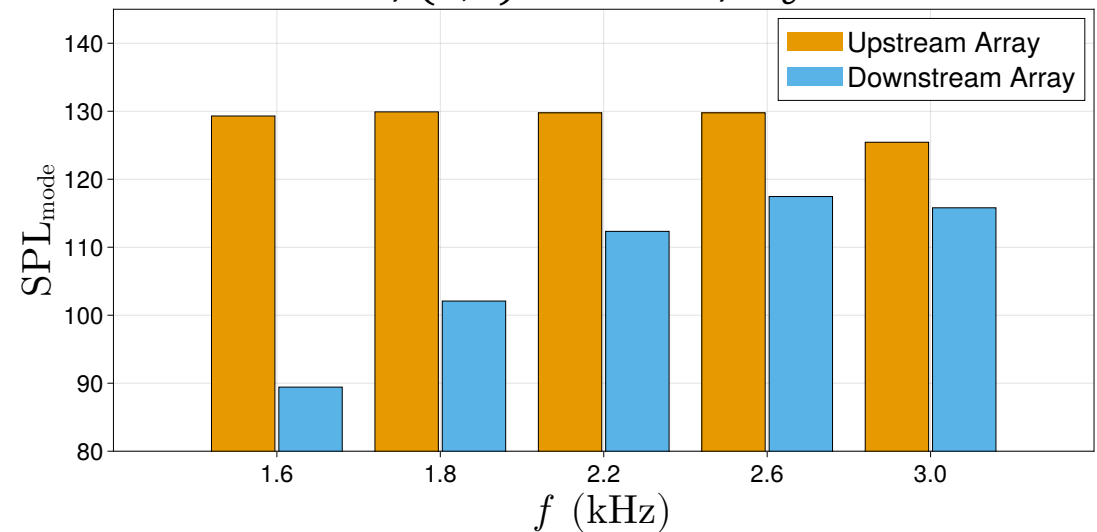
Avg. SPL difference in modes for CDTR3

PBE mode	CHE mode	$M_c = 0.1$	$M_c = 0.3$	$M_c = 0.5$
1	(0,0)	0.03	0.02	0.02
2	(1,0)	1.11	1.10	1.09
3	(2,0)	-0.26	-0.25	-0.12
4	(0,1)	1.23	1.38	1.44
5	(1,1)	2.27	2.35	2.32
6	(3,0)	-1.82	-1.83	-1.86

PBE, κ_4 dominant, $M_c = 0.5$



CHE, (0,1) dominant, $M_c = 0.5$





Summary and Future Work

Summary (Modal Structure)

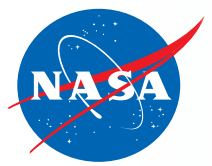
- Wavenumber deviation is only significant for negative modes at $M_c = 0.5$
- Lowest-order mode becomes increasingly non-planar as f and M_c increase
- Thus, a “plane-wave” component of the acoustic field may not exist under certain test conditions
- Asymmetry in positive and negative modes first appears for lowest-order mode
- This asymmetry can be drastic, as results at $f = 3000$ Hz and $M_c = 0.5$ show

Summary (Mode SPL)

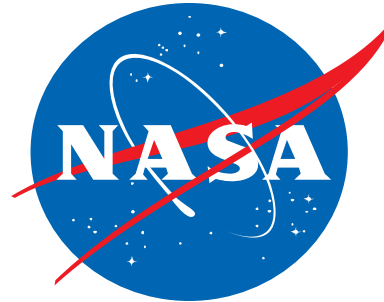
- Contrary to modal structure results, lowest-order mode appears least affected by shear flow (when looking purely at mode SPL)
- Insensitive to Mach number, not true for mode structure

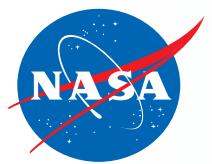
Future Work

- Extend mode decomposition to GFIT to examine higher frequencies
- Develop an impedance eduction procedure that incorporates 3D shear flow effects
- Support further flow direction studies and improved impedance optimization tools



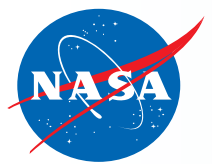
Questions?





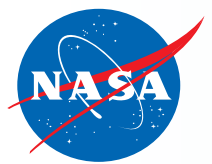
References

- [1] Ingard, U., “Influence of fluid motion past a plane boundary on sound reflection, absorption, and transmission,” *The Journal of the Acoustical Society of America*, Vol. 31, No. 7, 1959, pp. 1035–1036.
<https://doi.org/10.1121/1.1907805>.
- [2] Myers, M., “On the acoustic boundary condition in the presence of flow,” *Journal of Sound and Vibration*, Vol. 71, No. 3, 1980, pp. 429–434. [https://doi.org/10.1016/0022-460X\(80\)90424-1](https://doi.org/10.1016/0022-460X(80)90424-1).
- [3] Salikuddin, M., and Ramakrishnan, R., “Acoustic power measurement for single and annular stream duct-nozzle systems utilizing a modal decomposition scheme,” *Journal of Sound and Vibration*, Vol. 113, No. 3, 1987, pp. 441–472. [https://doi.org/10.1016/S0022-460X\(87\)80132-3](https://doi.org/10.1016/S0022-460X(87)80132-3).
- [4] Savkar, S., “Propagation of sound in ducts with shear flow,” *Journal of Sound and Vibration*, Vol. 19, No. 3, 1971, pp. 355–372. [https://doi.org/10.1016/0022-460X\(71\)90695-X](https://doi.org/10.1016/0022-460X(71)90695-X).
- [5] Nark, D. M., Jones, M. G., and Piot, E., “Assessment of axial wave number and mean flow uncertainty on acoustic liner impedance reduction,” 2018 AIAA/CEAS Aeroacoustics Conference, AIAA 2018-3444, Atlanta, Georgia, 2018. <https://doi.org/10.2514/6.2018-3444>.
- [6] Pridmore-Brown, D. C., “Sound propagation in a fluid flowing through an attenuating duct,” *Journal of Fluid Mechanics*, Vol. 4, No. 4, 1958, pp. 393–406. <https://doi.org/10.1017/S0022112058000537>.
- [7] Rienstra, S. W., “Numerical and asymptotic solutions of the Pridmore-Brown equation,” *AIAA Journal*, Vol. 58, No. 7, 2020, pp. 3001–3018. <https://doi.org/10.2514/1.J059140>.
- [8] Mehrmann, V., and Voss, H., “Nonlinear eigenvalue problems: a challenge for modern eigenvalue methods,” *GAMM-Mitteilungen*, Vol. 27, No. 2, 2004, pp. 121–152. <https://doi.org/10.1002/gamm.201490007>.

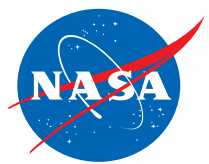


References

- [9] Ruhe, A., “Algorithms for the nonlinear eigenvalue problem,” SIAM Journal on Numerical Analysis, Vol. 10, No. 4, 1973, pp. 674–689. <https://doi.org/https://doi.org/10.1137/0710059>.



Backup Slides



Background: NASA LaRC Liner Technology Facility

High Intensity Modal Impedance Tube (HIMIT)

- Mach 0.0, SPL \leq 170 dB, Freq \leq **6 kHz**
- Tone and Broadband sources

Normal Incidence Tube (NIT)

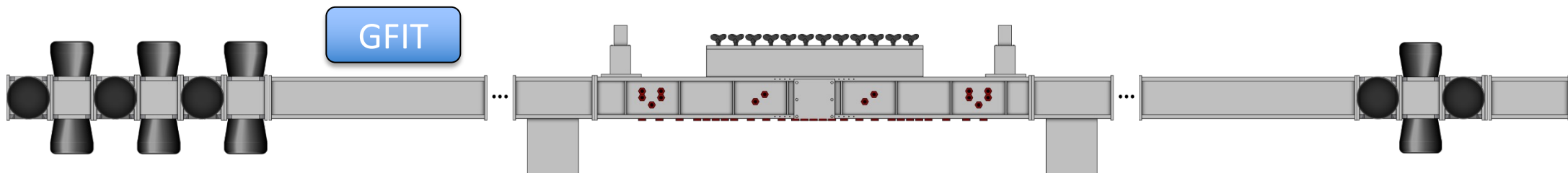
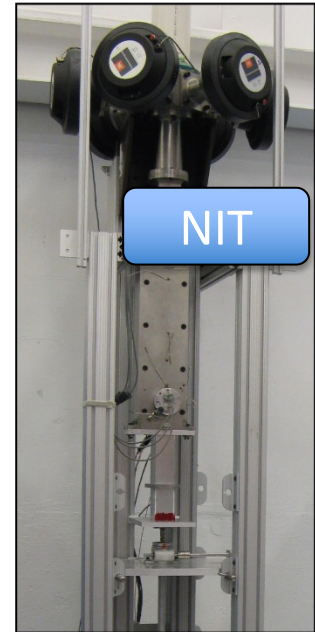
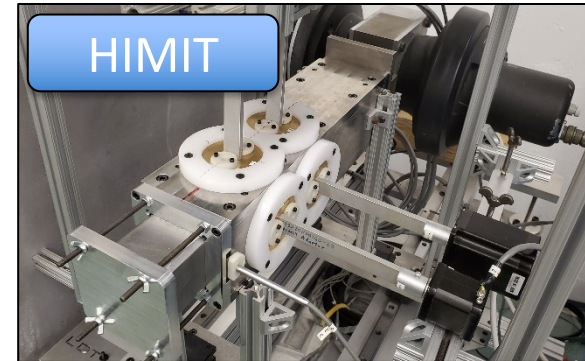
- Mach 0.0, SPL \leq 155 dB, Freq \leq 3 kHz
- Tone and Broadband sources

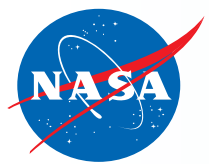
Grazing Flow Impedance Tube (GFIT)

- Mach \leq 0.6, SPL \leq 155 dB, Freq \leq **3 kHz**
- Tone source

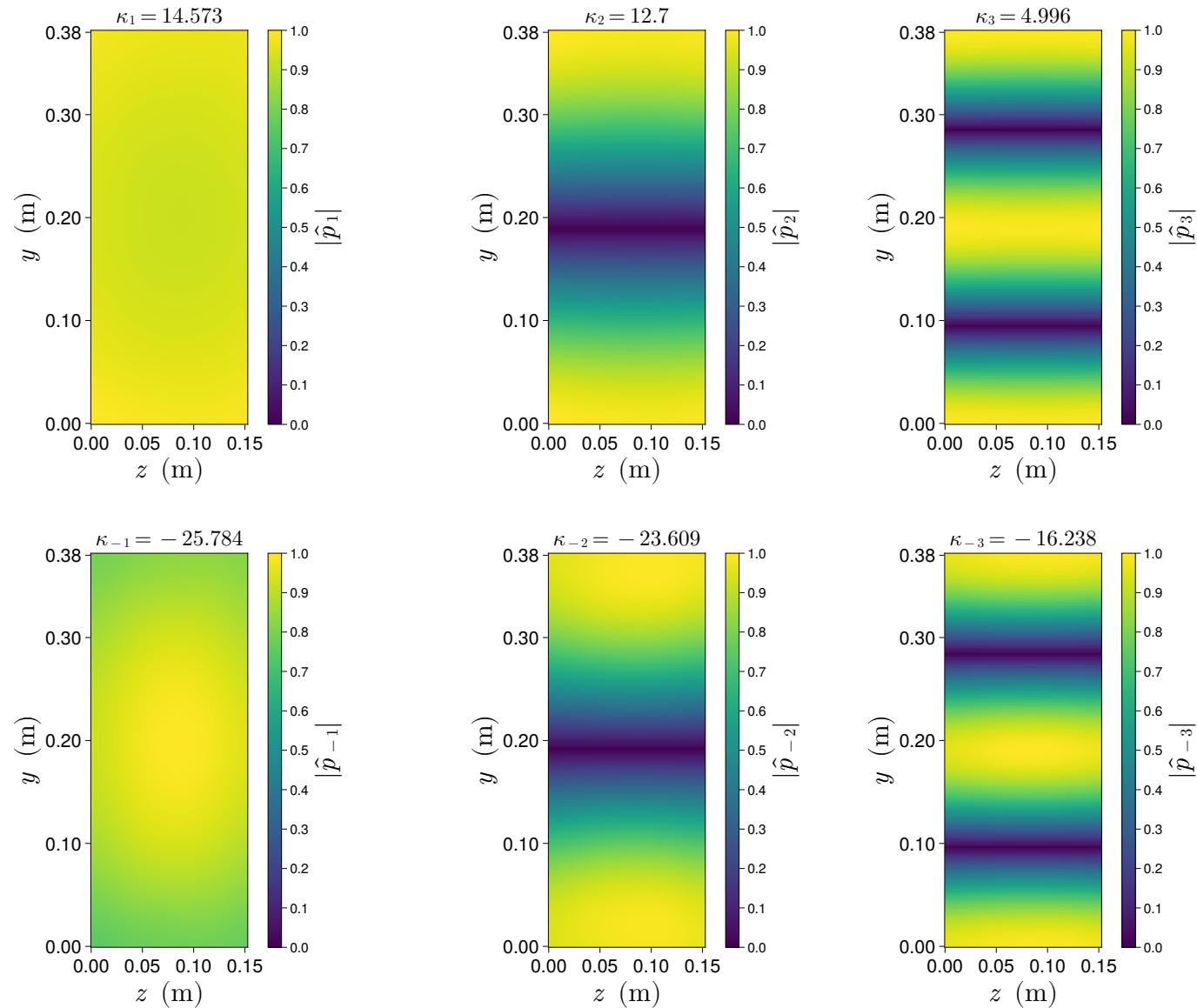
Curved Duct Test Rig (CDTR)

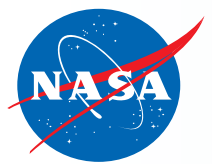
- Mach \leq 0.5, SPL \leq 135 dB, Freq \leq 3 kHz
- *Controlled* Tonal mode and Broadband sources





1000 Hz and Centerline Mach 0.3





Wavenumber Deviation Additional Info

- Implies a higher phase speed relative to CHE counterpart
- Reduction in angle of incidence, θ_i
- Propagation simulations based on PBE may indicate increased effectiveness of liner as compared to CHE

